Atmos. Chem. Phys. Discuss., doi:10.5194/acp-2015-939, 2016
Manuscript under review for journal Atmos. Chem. Phys.
Published: 18 January 2016

Atmospheric Chemistry and Physics Discussions

Characteristics of total gaseous mercury (TGM) concentrations in an industrial complex in southern Korea: Impacts from local sources

Yong-Seok Seo[1, 2], Seung-Pyo Jeong[1], Thomas M. Holsen[3], Young-Ji Han[4], Eunhwa Choi[5], Eun Ha Park[1], Tae Young Kim[1], Hee-Sang Eum[1], Dae Gun Park[1], Eunhye Kim[6], Soontae Kim[6], Jeong-Hun Kim[7], Jaewon Choi[8], Seung-Muk Yi[1, 2, *]

[1]Department of Environmental Health, Graduate School of Public Health, Seoul National University, 1 Gwanak, Gwanak-ro, Gwanak-gu, Seoul 151-742, South Korea

[2]Institute of Health and Environment, Seoul National University, 1 Gwanak, Gwanak-ro, Gwanak-gu, Seoul 151-742, South Korea

[3]Department of Civil and Environmental Engineering, Clarkson University, Potsdam, NY13699, USA

[4]Department of Environmental Science, Kangwon National University, 192-1, Hyoja-2-dong, Chuncheon, Kangwondo, 200-701, South Korea

[5]Asian Institute for Energy, Environment & Sustainability, Seoul National University, 1 Gwanak-ro, Gwanak-gu, Seoul 151-742, South Korea

[6]Department of Environmental, Civil and Transportation Engineering, Ajou University, Woncheon-dong, Yeongtong-gu, Suwon, 443-749, South Korea

[7]Division of Air Pollution Engineering, Department of Climate and Air Quality Research, National Institute of Environmental Research, Hwangyong-ro 42, Seogu, Incheon, 404-708, South Korea

[8]University of Pennsylvania, Philadelphia, PA19104, USA

[*]Address correspondence to Dr. Seung-Muk Yi, Graduate School of Public Health, Seoul National University, 1 Gwanak, Gwanak-ro, Gwanak-gu, Seoul 151-742, South Korea
E-mail) yiseung@snu.ac.kr
Telephone) 82-2-880-2736
Fax) 82-2-745-9104

Atmos. Chem. Phys. Discuss., doi:10.5194/acp-2015-939, 2016
Manuscript under review for journal Atmos. Chem. Phys.
Published: 18 January 2016

Atmospheric Chemistry and Physics Discussions

Abstract

Total gaseous mercury (TGM) concentrations were measured every 5 min in Pohang, Gyeongsangbuk-do, Korea during summer (17 August~23 August 2012), fall (9 October~17 October 2012), winter (22 January ~29 January 2013), and spring (26 March~3 April 2013) to: 1) characterize the hourly and seasonal variations of atmospheric TGM concentrations, 2) identify the relationships between TGM and co-pollutants, and 3) identify likely source directions and locations of TGM using conditional probability function (CPF), conditional bivariate probability function (CBPF) and total potential source contribution function (TPSCF).

The TGM concentration was statistically significantly highest in fall (6.7 ± 6.4 ng m^{-3}), followed by spring (4.8 ± 4.0 ng m^{-3}), winter (4.5 ± 3.2 ng m^{-3}) and summer (3.8 ± 3.9 ng m^{-3}). There was a statistically significant negative correlation between the TGM concentration and ambient air temperature *(r = -0.08) (p < 0.05).* Although the daytime temperature (14.7 ± 10.0 ºC) was statistically significantly higher than that in the nighttime (13.0 ± 9.8 ºC) (p < 0.05), the daytime TGM concentration (5.3 ± 4.7 ng m^{-3}) was statistically significantly higher than those in the nighttime (4.7 ± 4.7 ng m^{-3}) (p < 0.01), possibly due to local emissions related to industrial activities and activation of local surface emission sources. The observed ΔTGM/ΔCO was significantly lower than that of Asian long-range transport, but similar to that of local sources in Korea and in US industrial events suggesting that local sources are more important than that of long-range transport. CPF, CBPF and TPSCF indicated that the main sources of TGM were iron and manufacturing facilities, the hazardous waste incinerators and the coastal areas.

Atmos. Chem. Phys. Discuss., doi:10.5194/acp-2015-939, 2016
Manuscript under review for journal Atmos. Chem. Phys.
Published: 18 January 2016

Atmospheric Chemistry and Physics Discussions

67 **Keywords**: Total gaseous mercury (TGM); co-pollutant; conditional probability function
68 (CPF); conditional bivariate probability function (CBPF); total potential source contribution
69 function (TPSCF)

Atmos. Chem. Phys. Discuss., doi:10.5194/acp-2015-939, 2016
Manuscript under review for journal Atmos. Chem. Phys.
Published: 18 January 2016

Atmospheric Chemistry and Physics Discussions

1. Introduction

Mercury (Hg) in the atmosphere exists in three major inorganic forms including gaseous elemental mercury (GEM, Hg^0), gaseous oxidized mercury (GOM, Hg^{2+}) and particulate bound mercury (PBM, Hg(p)). GEM which is the dominant form of Hg in ambient air, (>95%) has a relatively long residence time (0.5~2 years) due to its low reactivity and solubility (Schroeder and Munthe, 1998). However, GOM has high water solubility and relatively strong surface adhesion properties (Han et al., 2005), so it has a short atmospheric residence time (~days). PBM is associated with airborne particles such as dust, soot, sea-salt aerosols, and ice crystals (Lu and Schroeder, 2004) and is likely produced, in part, by adsorption of GOM species such as $HgCl_2$ onto atmospheric particles (Gauchard et al., 2005; Lu and Schroeder, 2004; Sakata and Marumoto, 2005; Seo et al., 2015).

Atmospheric Hg is emitted from both natural sources (volcanoes, volatilization from aquatic and terrestrial environments) and anthropogenic sources (coal combustion, ferrous and non-ferrous metals manufacturing facilities, waste incineration and industrial boilers) (Lindberg et al., 2007; Pirrone et al., 2010; Schmeltz et al., 2011). Atmospheric Hg released from natural and anthropogenic sources leading to enhanced deposition (Mason and Sheu, 2002) can have impacts on terrestrial environments on local, regional and global scales (Lin and Pehkonen, 1999; Lindberg et al., 2007). Previous studies report that mercury directly released into terrestrial and aquatic ecosystems from industrial processes have influenced surface water, sediment and biological tissue (Flanders et al., 2010). Significant spatial variations in atmospheric Hg deposition near urban and industrial areas were due to local anthropogenic sources including municipal and waste incinerators, medical waste incinerators and cement kilns (Dvonch et al., 1998), ferrous and non-ferrous metal processing, incinerators, iron and steel manufacturing facilities, and oil and coal combustion (Hoyer et

Atmos. Chem. Phys. Discuss., doi:10.5194/acp-2015-939, 2016
Manuscript under review for journal Atmos. Chem. Phys.
Published: 18 January 2016

Atmospheric Chemistry and Physics Discussions

al., 1995) and coal combustion and waste incinerators (Iverfeldt, 1991). Miller et al. (2013) also reported that local sources of elemental Hg are typically industrial processes including retort facilities used in the mercury mining industry to convert Hg containing minerals to elemental Hg and chlor-alkali facilities.

Annual anthropogenic Hg emissions in South Korea have been estimated to be 12.8 tons; the major anthropogenic mercury emission sources are coal combustion in thermal power plants (25.8%), oil refineries (25.5%), cement kilns (21%), incinerators (19.3%) including sludge incinerators (4.7%), municipal waste incinerators (MWIs) (3%), industrial waste incinerators (IWIs) (2.7%), hospital/medical/infectious waste incinerators (HMIWIs) (8.8%), and iron manufacturing (7%) (Kim et al., 2010).

Receptor models are often used to identify sources of air pollutants and are focused on the pollutants behavior in the ambient environment at the point of impact (Hopke, 2003). In previous studies, conditional probability function (CPF), which utilizes the local wind direction, and potential source contribution function (PSCF), which utilizes longer backward trajectories (typically 3-5 days), combined with concentration information were used to identify possible transport pathways and source locations (Hopke, 2003). While PSCF has been used primarily to identify regional sources, it has also been used to identify local sources (Hsu et al., 2003). The objectives of this study were to characterize the hourly and seasonal variations of atmospheric TGM (the sum of the GEM and the GOM) concentrations, to identify the relationships between TGM and co-pollutant concentrations, and to identify likely source directions and locations of TGM using CPF, conditional bivariate probability function (CBPF) and total PSCF (TPSCF).

Atmos. Chem. Phys. Discuss., doi:10.5194/acp-2015-939, 2016
Manuscript under review for journal Atmos. Chem. Phys.
Published: 18 January 2016

Atmospheric Chemistry and Physics Discussions

2. Materials and methods

2.1. Sampling and analysis

TGM concentrations were measured on the roof of the Korean Federation of Community Credit Cooperatives (KFCCC) building (latitude: 35.992°, longitude: 129.404°, ~10 m above ground) in Pohang city, in Gyeongsangbuk-do, a province in eastern South Korea. Gyeongsangbuk-do has a population of 2.7 million (5% of the total population and the third most populated province in South Korea) and an area of 19,030 km^2 (19% of the total area of South Korea and the largest province geographically in South Korea).

Pohang city has a population of 500,000 (1% of the total population in South Korea) and an area of 605.4 km^2 (1.1% of the total area in South Korea). It is heavily industrialized with the third largest steel manufacturing facility in Asia and the fifth largest in the world. There are several iron and steel manufacturing facilities including electric and sintering furnaces using coking in Gyeongsangbuk-do including Pohang. In addition, there are several coke plants around the sampling site.

The Hyungsan River divides the city into a residential area and the steel complex. Hg emissions from iron and steel manufacturing, and a hazardous waste incinerator were estimated in a previous study (Kim et al., 2010) (Fig. 1).

TGM concentrations were measured every 5 min during summer (17 August~23 August 2012), fall (9 October~17 October 2012), winter (22 January ~29 January 2013), and spring (26 March~3 April 2013) using a mercury vapor analyzer (Tekran 2537B) which has two gold cartridges that alternately collect and thermally desorb mercury. Ambient air at a flow rate of 1.5 L min^{-1} was transported through a 3 m-long heated sampling line in to the analyzer.

Atmos. Chem. Phys. Discuss., doi:10.5194/acp-2015-939, 2016
Manuscript under review for journal Atmos. Chem. Phys.
Published: 18 January 2016

2.2. Meteorological data

Meteorological data (air temperature, relative humidity, and wind speed and direction) were obtained from the Automatic Weather Station (AWS) operated by the Korea Meteorological Administration (KMA) (6 km from the site). Hourly concentrations of NO_2, O_3, CO, PM_{10} and SO_2 were obtained from the National Air Quality Monitoring Network (NAQMN) (3 km from the site) (Fig. 1). Fig. S1 shows the frequency of counts of measured wind direction occurrence by season during the sampling period. The predominant wind direction at the sampling site was W (20.9%) and WS (19.2%), and calm conditions of wind speed less than 1 m s^{-1} occurred 7.6% of the time during the sampling period. Compared to other seasons, however, the prevailing winds in summer were N (17.0%), NE (16.4%), S (16.4%), and SW (15.8%).

2.3. QA/QC

Automated daily calibrations were carried out for the Tekran 2537B using an internal permeation source. Two-point calibrations (zero and span) were separately performed for each gold cartridge. Manual injections were used to evaluate these automated calibrations using a saturated mercury vapor standard. The relative percent difference (RPD) between automated calibrations and manual injections was less than 2%. The recovery measured by directly injecting known amounts of four mercury vapor standards when the sample line was connected to zero air ranged from 92 to 110% (99.4 ± 5.2% in average).

3. Model descriptions

3.1. Conditional Probability Function (CPF)

Atmos. Chem. Phys. Discuss., doi:10.5194/acp-2015-939, 2016
Manuscript under review for journal Atmos. Chem. Phys.
Published: 18 January 2016

Atmospheric Chemistry and Physics Discussions

Conditional Probability Function (CPF) was originally performed to determine which wind directions dominate during high concentration events to evaluate local source impacts (Ashbaugh et al., 1985). It has been successfully used in many previous studies (Begum et al., 2004; Kim et al., 2003a; Kim et al., 2003b; Xie and Berkowitz, 2006; Zhao et al., 2004; Zhou et al., 2004). CPF estimates the probability that the source contribution from a given wind direction will exceed the threshold criterion. The CPF is defined as follows Eq. (1).

$$CPF_{\Delta\theta} = \frac{m_{\Delta\theta}|_{C \geq x}}{n_{\Delta\theta}} \quad (1)$$

where, $m_{\Delta\theta}$ is the number of samples from the wind sector θ having concentration C greater than or equal to a threshold value x, and $n_{\Delta\theta}$ is the total number of samples from wind sector $\Delta\theta$. In this study, 16 sectors ($\Delta\theta$ = 22.5º) were used and calm winds (≤ 1 m s^{-1}) were excluded from the analysis. The threshold criterion was set at above the overall average TGM concentration (5.0 ng m^{-3}). Thus, CPF indicates the potential for winds from a specific direction to contribute to high air pollution concentrations.

3.2. Conditional Bivariate Probability Function (CBPF)

CBPF couples ordinary CPF with wind speed as a third variable, allocating the measured concentration of pollutant to cells defined by ranges of wind direction and wind speed rather than to only wind direction sectors. CBPF also considers the full distribution of concentrations rather than concentrations exceeding a threshold and can identify unknown contributions from different sources with different dispersion characteristics.

The CBPF is defined as follows Eq. (2).

Atmos. Chem. Phys. Discuss., doi:10.5194/acp-2015-939, 2016
Manuscript under review for journal Atmos. Chem. Phys.
Published: 18 January 2016

Atmospheric Chemistry and Physics Discussions

187

188 $$CBPF_{\Delta\theta,\Delta u} = \frac{m_{\Delta\theta,\Delta u|C\geq x}}{n_{\Delta\theta,\Delta u}} \quad (2)$$

189

190 where, $m_{\Delta\theta,\Delta u}$ is the number of samples in the wind sector $\Delta\theta$ with wind speed interval Δu
191 having concentration *C* greater than a threshold value *x*, and $n_{\Delta\theta\Delta u}$ is the total number of
192 samples in that wind direction-speed interval. The threshold criterion was set at above the
193 overall average TGM concentration (5.0 ng m^{-3}). The extension to the bivariate case provides
194 more information on the nature of the sources because different source types can have
195 different wind speed dependencies. More detailed information is described in a previous
196 study (Uria-Tellaetxe and Carslaw, 2014).

197

198 *3.3. Potential Source Contribution Function (PSCF)*

199 The PSCF model has been extensively and successfully used in the previous studies to
200 identify the likely source areas (Cheng et al., 1993; Han et al., 2004; Hopke et al., 2005; Lai
201 et al., 2007; Lim et al., 2001; Poissant, 1999; Zeng and Hopke, 1989). PSCF which was
202 developed by Ashbaugh et al. (1985) is a simple method that links residence time in upwind
203 areas with high concentrations through a conditional probability field. $PSCF_{ij}$ is the
204 conditional probability that an air parcel that passed through the *ij*th cell had a high
205 concentration upon arrival at the monitoring site and is defined in the following Eq. (3).

206

207 $$PSCF_{ij} = \frac{m_{ij}}{n_{ij}} \quad (3)$$

208

Atmos. Chem. Phys. Discuss., doi:10.5194/acp-2015-939, 2016
Manuscript under review for journal Atmos. Chem. Phys.
Published: 18 January 2016

Atmospheric Chemistry and Physics Discussions

where, n_{ij} is the number of trajectory segment endpoints that fall into the *ij*-th cell, and m_{ij} is the number of segment endpoints in the same grid cell (*ij*-th cell) when the concentrations are higher than a criterion value as measured at the sampling site. High PSCF value grid cells are regarded as possible source locations. Cells including emission sources can be identified with conditional probabilities close to one if trajectories that have crossed the cells efficiently transport the released pollutant to the receptor site. Therefore, the PSCF model provides a tool to map the source potentials of geographical areas.

The criterion value of PSCF for TGM concentration was set at above the overall average concentration (5.0 ng m^{-3}) to identify the emission sources associated with high TGM concentrations and provide a better estimation and resolution of source locations during the sampling periods. The geographic area covered by the computed trajectories was divided into an array of 0.05º latitude by 0.05º longitude grid cells. In this study, 24hr backward trajectories starting at every hour at a height of 10, 50, and 100 m above ground level were computed using the vertical velocity model. Each trajectory was terminated if they exit the model top (5,000m), but advection continues along the surface if trajectories intersect the ground. To generate horizontally highly resolved meteorological inputs for trajectory calculations, the Weather Research and Forecast (WRF) model was used to generate a coarse domain at a resolution of 27 km and a nested domain at a horizontal resolution of 9 km, which geographically covers northeast Asia and the southern part of the Korean Peninsula, respectively. The nested domain has 174 columns in the east-west direction and 114 rows in the north-south direction. PSCF was calculated with 9 km meteorology data.

In this study, TPSCF was used at different starting heights (10m, 50m, and 100m above ground level) since backward trajectories starting at different heights traverse different

Atmos. Chem. Phys. Discuss., doi:10.5194/acp-2015-939, 2016
Manuscript under review for journal Atmos. Chem. Phys.
Published: 18 January 2016

Atmospheric Chemistry and Physics Discussions

232 distances and pathways, thus providing information that cannot be obtained from a single
233 starting height (Cheng et al., 1993).
234 Generally, PSCF results show that the potential sources covered wide areas instead of
235 indicating individual sources due to the trailing effect. The trailing effect appears since PSCF
236 distributes a constant weight along the path of the trajectories. To minimize the effect of
237 small n_{ij} values, resulting in high TPSCF values with high uncertainties, an arbitrary weight
238 function $W(n_{ij})$ was applied to down-weight the PSCF values for the cell in which the total
239 number of end points was less than three times the average value of the end points (Choi et
240 al., 2011; Heo et al., 2009; Hopke et al., 1995; Polissar et al., 2001). The TPSCF value for a
241 grid cell was defined with following Eq. (4).
242

243 $$P(TPSCF_{ij}) = \frac{P(m_{ij})_{10m} + P(m_{ij})_{50m} + P(m_{ij})_{100m}}{P(n_{ij})_{10m} + P(n_{ij})_{50m} + P(n_{ij})_{100m}} \times W \quad (4)$$

244
245 where,

246 $$W(n_{ij}) = \begin{cases} 1.0, & 3n_{ave} < n_{ij} \\ 0.8, & 2n_{ave} < n_{ij} \le 3n_{ave} \\ 0.6, & n_{ave} < n_{ij} \le 2n_{ave} \\ 0.4, & 0.5n_{ave} < n_{ij} \le n_{ave} \\ 0.2, & n_{ij} \le 0.5n_{ave} \end{cases}$$

247
248 **4. Clean Air Policy Support System (CAPSS) data**
249 In this study, the Korean National Emission Inventory estimated using Clean Air Policy
250 Support System (CAPSS) data developed by the National Institute of Environmental

Atmos. Chem. Phys. Discuss., doi:10.5194/acp-2015-939, 2016
Manuscript under review for journal Atmos. Chem. Phys.
Published: 18 January 2016

Atmospheric Chemistry and Physics Discussions

Research (NIER) were used (http://airemiss.nier.go.kr/main.jsp (accessed December 09, 2015)). The CAPSS is the national emission inventory system for the air pollutants (CO, NOx, SOx, TSP, PM_{10}, $PM_{2.5}$, VOCs and NH_3) which utilizes various national, regional and local statistical data collected from about 150 organizations in Korea. In CAPSS, the Source Classification Category (SCC) excluding fugitive dust and biomass burning based on the European Environment Agency's (EEA) CORe Inventory of AIR emissions was classified into the following four levels (EMEP/CORINAIR) (NIER, 2011).

(1) The upper level (SCC1): 11 source categories ,

(2) The intermediate level (SCC2): 42 source categories and

(3) The lower level (SCC3): 173 source categories

The sectoral contributions of emissions of South Korea, Gyeongsangbuk-do and Pohang for CO, NOx, SOx, TSP, PM_{10}, $PM_{2.5}$, VOC and NH_3 are shown in Fig. S2 (See SI for details).

More detailed information about SCCs in CAPSS is described in Table S1.

5. Results and Discussions

5.1. General characteristics of TGM

The seasonal distributions of TGM were characterized by large variability during each sampling period (Fig. 2). The average concentration of TGM during the complete sampling period was 5.0 ± 4.7 ng m^{-3} (range: 1.0-79.6 ng m^{-3}). This is significantly higher than the Northern Hemisphere background concentration (~1.5 ng m^{-3}) (Sprovieri et al., 2010) and those measured in Japan and other locations in Korea, however considerably lower than those

Atmos. Chem. Phys. Discuss., doi:10.5194/acp-2015-939, 2016
Manuscript under review for journal Atmos. Chem. Phys.
Published: 18 January 2016

Atmospheric Chemistry and Physics Discussions

measured near large Hg sources in China (Table 1). The median TGM concentration was 3.6 ng m^{-3} which was much lower than that of the average, suggesting that there were some extreme pollution episodes with very high TGM concentrations.

The TGM concentration follows a typical log-normal distribution (Fig. S3). The range of 2 to 5 ng m^{-3} dominated the distribution, accounting for more than half of the total number of samples (60.8%). The maximum frequency of 28.1% occurred between 2 and 3 ng m^{-3}. Extremely high TGM concentration events (>20 ng m^{-3}) were also observed (1.7% of the time).

5.2. Seasonal variation

The TGM concentration was statistically significantly higher in fall (6.7 ± 6.4 ng m^{-3}) (p < 0.01), followed by spring (4.8 ± 4.0 ng m^{-3}), winter (4.5 ± 3.2 ng m^{-3}) and summer (3.8 ± 3.9 ng m^{-3}) (Table 2). The highest concentrations (TGM > 10 ng m^{-3}) were measured more frequently in fall (24.7%), and the lowest concentrations (TGM < 3 ng m^{-3}) mainly occurred in summer (49.7%). The low TGM concentration in summer is likely because increased mixing height (Friedli et al., 2011), and gas phase oxidation (Choi et al., 2013; Huang et al., 2010; Lynam and Keeler, 2006) at higher temperatures particularly at this sampling site which is close to the ocean (2 km) where oxidation involving halogens may be enhanced (Holmes et al., 2009; Lin et al., 2006). As will be discussed later, the high TGM concentrations in fall was due to different wind direction (see Fig. S1) and sources.

The average concentrations of NO_2, O_3, CO, PM_{10} and SO_2 during the complete sampling period were 23.1 ± 10.8 ppbv, 24.6 ± 12.5 ppbv, 673.7 ± 487.3 ppbv, 55.5 ± 26.4 μg m^{-3} and 6.7 ± 4.3 ppbv, respectively. NO_2, O_3, CO, PM_{10} and SO_2 concentrations were highest in spring (Table 2). There was a statistically significant positive correlation between the TGM

Atmos. Chem. Phys. Discuss., doi:10.5194/acp-2015-939, 2016
Manuscript under review for journal Atmos. Chem. Phys.
Published: 18 January 2016

Atmospheric Chemistry and Physics Discussions

299 and PM_{10} (r = 0.10) ($p < 0.01$). However, the TGM concentration was not significantly
300 correlated with NO_2, CO or SO_2 concentrations. Previous studies reported that the high
301 concentrations of NO_2, CO and SO_2 were likely due to combustion sources associated with
302 space heating (Choi et al., 2009).
303
304 *5.3. Relationship between TGM and CO*
305 CO has a significant anthropogenic source and is considered to be an indicator of
306 anthropogenic emissions (Mao et al., 2008). Previous studies reported that TGM and CO
307 have a strong correlation because they have similar emission sources (combustion processes)
308 and similar long atmospheric residence times (Weiss-Penzias et al., 2003).
309 There was a weak positive correlation between TGM and CO in this study (r = 0.04) (p =
310 0.27). However there was a statistically significant correlation between TGM and CO in
311 winter (r = 0.25) ($p < 0.05$), suggesting that TGM and CO were affected by similar, possibly
312 distant, anthropogenic emission sources in winter.
313 However, there were no statistically significant correlations between TGM and CO in
314 spring (r = 0.02) ($p = 0.78$), in summer (r = 0.13) ($p = 0.08$), or in fall (r = -0.03) ($p = 0.69$)
315 (Fig. S4), indicating that TGM and CO were affected by different anthropogenic emission
316 sources in these seasons.
317 Previous studies identified the long-range transport of mercury using the ΔTGM/ΔCO
318 enhancement ratio (Choi et al., 2009; Jaffe et al., 2005; Kim et al., 2009; Weiss-Penzias et al.,
319 2003; Weiss-Penzias et al., 2006). Kim et al. (2009) and Choi et al. (2009) investigated high
320 concentration events which were defined as at least a 10 h period with hourly average TGM
321 and CO concentrations higher than the average monthly TGM and CO concentrations. They
322 reported that long-range transport events were characterized by high values of TGM/CO ratio

Atmos. Chem. Phys. Discuss., doi:10.5194/acp-2015-939, 2016
Manuscript under review for journal Atmos. Chem. Phys.
Published: 18 January 2016

Atmospheric Chemistry and Physics Discussions

323 (ΔTGM/ΔCO) (0.0052-0.0158 ng m^{-3} ppb^{-1}) and high correlations (r^2>0.5), whereas local
324 events showed low ΔTGM/ΔCO (0.0005 ng m^{-3} ppb^{-1} in average) and weak correlations (r^2 <
325 0.5).
326 The observed ΔTGM/ΔCO was 0.0001 ng m^{-3} ppb^{-1} in spring, 0.0005 ng m^{-3} ppb^{-1} in
327 summer, -0.0007 ng m^{-3} ppb^{-1} in fall, 0.0011 ng m^{-3} ppb^{-1} in winter, which are significantly
328 lower than that indicative of Asian long-range transport (0.0046-0.0056 ng m^{-3} ppb^{-1}) (Friedli
329 et al., 2004; Jaffe et al., 2005; Weiss-Penzias et al., 2006), suggesting that local sources are
330 more important than that of long-range transport in this study. The ΔTGM/ΔCO in winter
331 (0.0011 ng m^{-3} ppb^{-1}) was similar to that of a site impacted by local sources in Korea (Kim et
332 al., 2009) and in US industrially related events (0.0011 ng m^{-3} ppb^{-1}) (Weiss-Penzias et al.,
333 2007).
334
335 *5.4. Diurnal variations*
336 Diurnal variations of TGM (Fig. 3), co-pollutants concentrations, and meteorological
337 data were observed (Fig. S5). TGM, O_3, CO, SO_2, and temperature in the daytime were
338 statistically significantly higher than those in the nighttime (p < 0.05) except PM_{10} (p = 0.09)
339 (Fig. S6). However, NO_2 during the nighttime because of relatively lower photochemical
340 reactivity with O_3 was statistically significantly higher than that in daytime (p < 0.05)
341 (Adame et al., 2012). TGM generally showed a consistent diurnal variation with a maximum
342 in the early morning (06:00-09:00) and minimum in the afternoon (14:00-17:00), similar to
343 previous studies (Dommergue et al., 2002; Friedli et al., 2011; Li et al., 2011; Liu et al.,
344 2011; Mao et al., 2008; Shon et al., 2005; Song et al., 2009; Stamenkovic et al., 2007).

Atmos. Chem. Phys. Discuss., doi:10.5194/acp-2015-939, 2016
Manuscript under review for journal Atmos. Chem. Phys.
Published: 18 January 2016

345 The daytime TGM concentration (5.3 ± 4.7 ng m^{-3}) was statistically significantly higher
346 than that in nighttime (4.7 ± 4.7 ng m^{-3}) ($p < 0.01$), which was similar to several previous
347 studies (Cheng et al., 2014; Stamenkovic et al., 2007) but different than others (Lee et al.,
348 1998; Nakagawa, 1995).
349 In a previous study the daytime TGM concentrations was relatively lower than that in
350 the nighttime because the sea breeze transported air containing low amounts of TGM from
351 the ocean during the daytime whereas the land breeze transported air containing relatively
352 high concentrations of TGM from an urban area during the nighttime (Kellerhals et al.,
353 2003). As will be discussed later, this is possibly due to local emission sources because the
354 daytime temperature (14.7 ± 10.0 ºC) was statistically significantly higher than that in the
355 nighttime (13.0 ± 9.8 ºC) (t-test, $p < 0.05$) and there was a statistically significant negative
356 correlation between TGM concentration and ambient air temperature ($p < 0.05$).
357 As shown in Fig. 3 and Fig. S5, there was a negative relationship between the TGM
358 concentrations and O_3 concentrations (r = -0.18) ($p < 0.01$), suggesting that oxidation of
359 GEM in the oxidizing atmosphere during periods of strong atmospheric mixing was partially
360 responsible for the diurnal variations of TGM concentrations. In addition, oxidation of GEM
361 by bromine species in the coastal area (Obrist et al., 2011) or by chloride radicals in marine
362 boundary layer (Laurier et al., 2003) might play a significant role.
363 Significantly different diurnal patterns have been observed at many suburban sites with
364 the daily maximum occurring in the afternoon (12:00-15:00), possibly due to local emission
365 sources and transport (Fu et al., 2010; Fu et al., 2008; Kuo et al., 2006; Wan et al., 2009).
366 Other studies in Europe reported that TGM concentrations were relatively higher early in the
367 morning or at night possibly due to mercury emissions from surface sources that accumulated
368 in the nocturnal inversion layer (Lee et al., 1998; Schmolke et al., 1999).

Atmos. Chem. Phys. Discuss., doi:10.5194/acp-2015-939, 2016
Manuscript under review for journal Atmos. Chem. Phys.
Published: 18 January 2016

There was a statistically significant negative correlation between the TGM concentration and ambient air temperature ($p < 0.05$). High ambient air temperature in the daytime will increase the height of the boundary layer and dilute the TGM, and the relatively lower boundary layer at nighttime could concentrate the TGM in the atmosphere (Li et al., 2011). Although there was a statistically significant negative correlation between the TGM concentration and ambient air temperature, there was a rapid increase in TGM concentration between 06:00-09:00 when ambient temperatures also increased possibly due to local emissions related to industrial activities, increased traffic, and activation of local surface emission sources. Similar patterns were found in previous studies (Li et al., 2011; Stamenkovic et al., 2007).

5.5. CPF, CBPF and TPSCF results of TGM

Based on the above results, the diurnal variations in TGM concentration are due to a combination of: 1) reactions with an oxidizing atmosphere, 2) changes in ambient temperature and 3) local emissions related to industrial activities. To supplement these conclusions CPF and CBPF were used to identify source directions and TPSCF was used to identify potential source locations.

Conventional CPF, CBPF and TPSCF plots for TGM concentrations higher than the average concentration show high source probabilities to the west in the direction of large steel manufacturing facilities and waste incinerators (Fig. 4). The CPF only shows high probabilities from the west and provides no further information, however, the CBPF shows groups of sources with the high probabilities from the west and the northeast. CBPF shows that the high probabilities from the west occurred under high wind speed as well as low wind

Atmos. Chem. Phys. Discuss., doi:10.5194/acp-2015-939, 2016
Manuscript under review for journal Atmos. Chem. Phys.
Published: 18 January 2016

Atmospheric Chemistry and Physics Discussions

speed, suggesting that there are not only emissions from stacks but also non-buoyant ground level sources (Uria-Tellaetxe and Carslaw, 2014).

TPSCF identified the likely sources of TGM as the iron and manufacturing facilities and the hazardous waste incinerators which are located to the west from the sampling site. A previous study reported that the waste incinerators (9%) and iron and steel manufacturing (7%) were relatively high Hg emissions sources in Korea (Kim et al., 2010). Waste incinerators emissions were due to the high Hg content in the waste (Lee et al., 2004). Emissions from iron and steel manufacturing are due to the numerous electric and sintering furnaces using coking which emits relatively high mercury concentrations (Lee et al., 2004) in Gyeongsangbuk-do including Pohang. There are several coke plants around the sampling site (http://www.poscoenc.com/upload/W/BUSINESS/PDF/ENG_PLANT_2_1_3_5.pdf (accessed December 09, 2015)). They are essential parts of the iron and steel manufacturing, and the major source of atmospheric mercury related to the iron and steel manufacturing is from coke production (Pacyna et al., 2006).

The coastal areas east of the sampling site where there are large ports were also identified as the likely source areas of TGM. A previous study reported that the emissions of gaseous and particulate pollutants were high during vehicular operations in port areas and from marine vessel and launches (Gupta et al., 2002). Another possibility is that significant amount of GEM are emitted from the ocean surface because of photo-chemically and microbiologically mediated photo-reduction of dissolved GOM (Amyot et al., 1994; Zhang and Lindberg, 2001). The East Sea was also identified as potential source areas likely because this is an area with lots of domestic passenger ships routes.

Atmos. Chem. Phys. Discuss., doi:10.5194/acp-2015-939, 2016
Manuscript under review for journal Atmos. Chem. Phys.
Published: 18 January 2016

Atmospheric Chemistry and Physics Discussions

Conclusions

During the sampling periods, the average TGM concentration was higher than the Northern Hemisphere background concentration, however, considerably lower than those near industrial areas in China and higher than those in Japan and other locations in Korea. The median concentration of TGM was much lower than that of the average, suggesting that there were some extreme pollution episodes with very high TGM concentrations. The TGM concentration was highest in fall, followed by spring, winter and summer. The high TGM concentration in fall is due to transport from different wind directions than during the other periods. The low TGM concentration in summer is likely due to increased mixing height and gas phase oxidation at higher temperatures particularly at this sampling site which is close to the ocean (2 km) where oxidation involving halogens may be enhanced.

TGM consistently showed a diurnal variation with a maximum in the early morning (06:00-09:00) and minimum in the afternoon (14:00-17:00). Although there was a statistically significant negative correlation between the TGM concentration and ambient air temperature, the daytime TGM concentration was higher than those in the nighttime, suggesting that local emission sources are important. There was a negative relationship between the TGM concentrations and O_3 concentrations, indicating that the oxidation was partially responsible for the diurnal variations of TGM concentrations. The observed $\Delta TGM/\Delta CO$ was significantly lower than that indicative of Asian long-range transport, suggesting that local sources are more important than that of long-range transport. CPF, CBPF and JP-PSCF indicated that the main sources of TGM were the iron and manufacturing facilities, the hazardous waste incinerators and the coastal areas. The East Sea was also identified as likely source areas because this is an area with lots of domestic passenger ships routes.

Atmos. Chem. Phys. Discuss., doi:10.5194/acp-2015-939, 2016
Manuscript under review for journal Atmos. Chem. Phys.
Published: 18 January 2016

Author contribution

Yong-Seok Seo conducted a design of the study, the experiments and analysis of data, wrote the initial manuscript, and finally approved the final manuscript. Seung-Pyo Jeong, Eun Ha Park, Tae Young Kim, Hee-Sang Eum, Dae Gun Park, Eunhye Kim, Jaewon Choi and Jeong-Hun Kim conducted the experiments, analysis of data, and finally approved the final manuscript. Thomas M. Holsen, Young-Ji Han and Eunhwa Choi and Soontae Kim conducted interpretation of the results, revision of the initial manuscript, and finally approved the final manuscript. Seung-Muk Yi conducted a design of the study, acquisition of data of the study, interpretation of data, and revision of the initial manuscript, and finally approved the final manuscript.

Acknowledgments

We thank National Institute of Environmental Research (NIER) for providing CAPSS data. This work was supported by Brain Korea 21 (BK21) Plus Project (Center for Healthy Environment Education and Research) through the National Research Foundation (NRF) of Korea and Korea Ministry of Environment (MOE) as “the Environmental Health Action Program”.

Atmos. Chem. Phys. Discuss., doi:10.5194/acp-2015-939, 2016
Manuscript under review for journal Atmos. Chem. Phys.
Published: 18 January 2016

456 **Table List**

460

461 **Figure List**

Atmos. Chem. Phys. Discuss., doi:10.5194/acp-2015-939, 2016
Manuscript under review for journal Atmos. Chem. Phys.
Published: 18 January 2016

467 **Table 1.** Comparison with previous studies for TGM concentrations.

Country	Location	Sampling period	TGM conc. (ng m^{-3})	Classifications	Reference
China	Nanjing, Jiangsu	Jan. 2011 ~ Dec. 2011	7.9	Urban	Zhu et al. (2012)
China	Guangzhou, Guangdong	Jul. 1999 ~ Jul. 2000	13.5 - 25.4	Urban	Fang et al. (2004)
China	Gui Yang, Guizhou	Jan. 2010 ~ Feb. 2010	8.4	Urban	Feng et al. (2004)
China	Changchun, Jilin	Sep. 1999 ~ Aug. 2000	9.1-15.4	Suburban	Fang et al. (2004)
Japan	Tokyo	Apr. 2000 ~ Mar. 2001	2.7	Urban	Sakata and Marumoto (2002)
Japan	Tokai-mura	Oct. 2005 ~ Aug. 2006	3.8	Suburban	Osawa et al. (2007)
Korea	Seoul	19 Sep. 1997 ~ 29 Sep. 1997 27 May. 1998 ~ 18 Jun. 1998	3.6	Urban	Kim and Kim (2001)
Korea	Seoul	Feb. 2005 ~ Feb. 2006	3.2	Urban	Kim et al. (2009)
Korea	Seoul	Feb. 2005 ~ Dec. 2006	3.4	Urban	Choi et al. (2009)
Korea	Gyeongsangbuk-do, Pohang	17 Aug. 2012 ~ 23 Aug. 2012 9 Oct. 2012 ~ 17 Oct. 2012 22 Jan. 2013 ~ 29 Jan. 2013 26 Mar. 2013 ~ 3 Apr. 2013	5.0	Urban	This study

468

469

Atmos. Chem. Phys. Discuss., doi:10.5194/acp-2015-939, 2016
Manuscript under review for journal Atmos. Chem. Phys.
Published: 18 January 2016

Atmospheric Chemistry and Physics Discussions

Table 2. Summary of atmospheric concentrations of TGM and co-pollutants, and meteorological data. Note that TGM was measured every 5-min, and other pollutants and meteorological data were measured every 1-hour.

		TGM (ng m^{-3})	NO_2 (ppb)	O_3 (ppb)	CO (ppb)	PM_{10} (μg m^{-3})	SO_2 (ppb)	Temperature (℃)	Wind speed (m s^{-1})	Humidity (%)	Solar radiation (MJ m^{-2})
Spring	**N**	2139	189	215	215	215	215	216	216	216	216
	Average	4.8 ± 4.0	25.3 ± 9.0	29.4 ± 14.2	766.5 ± 505.2	70.1 ± 26.0	7.6 ± 3.8	10.5 ± 4.2	2.2 ± 1.2	56.2 ± 16.8	0.82 ± 1.09
	Range	1.9 – 45.3	8 – 55	2 – 58	300 – 3100	28 - 204	5 - 35	1.1 – 21.6	0.4 – 6.2	19.0 – 94.0	0 – 3.44
Summer	**N**	1863	187	188	187	188	188	186	180	186	141
	Average	3.8 ± 3.9	18.3 ± 9.2	18.9 ± 10.1	697.3 ± 689.7	35.1 ± 15.8	6.5 ± 6.2	26.6 ± 4.2	2.2 ± 1.1	82.5 ± 13.9	0.40 ± 0.69
	Range	1.2 – 75.9	4 – 44	5 – 48	200 – 3300	12 – 87	2 - 27	19.7 – 34.1	0.1 – 6.4	43 - 98	0 – 2.92
Fall	**N**	2226	212	212	212	212	211	216	216	216	216
	Average	6.7 ± 6.4	25.0 ± 7.8	23.7 ± 13.1	662.7 ± 350.2	58.1 ± 17.8	5.3 ± 3.5	17.4 ± 3.2	2.1 ± 0.8	54.5 ± 14.7	0.62 ± 0.90
	Range	1.0 – 79.6	9 – 53	6 – 69	300 – 2900	20 - 145	3 - 39	11.7 – 25.2	0.5 – 4.5	12 - 79	0 – 2.90
Winter	**N**	1917	188	187	188	188	186	192	192	192	192
	Average	4.5 ± 3.2	23.5 ± 14.7	26.1 ± 8.7	556.4 ± 298.9	56.3 ± 30.5	7.4 ± 2.5	1.1 ± 4.3	2.8 ± 1.1	46.3 ± 24.5	0.43 ± 0.71
	Range	1.3 – 66.4	5 – 74	1 – 41	200 – 2400	18 – 161	5 – 24	-0.65 – 10.1	0.5 – 6.0	11 - 90	0 – 2.34
Total	**N**	8145	776	802	802	803	800	810	804	810	765
	Average	5.0 ± 4.7	23.1 ± 10.8	24.6 ± 12.5	673.7 ± 487.3	55.5 ± 26.4	6.7 ± 4.3	13.8 ± 9.9	2.3 ± 1.1	59.4 ± 22.1	0.59 ± 0.90
	Range	1.0 – 79.6	4 – 74	1 – 69	200 – 3300	12 – 204	2 – 39	-6.5 – 34.1	0.1 – 6.4	11 - 98	0 – 3.44

Atmos. Chem. Phys. Discuss., doi:10.5194/acp-2015-939, 2016
Manuscript under review for journal Atmos. Chem. Phys.
Published: 18 January 2016

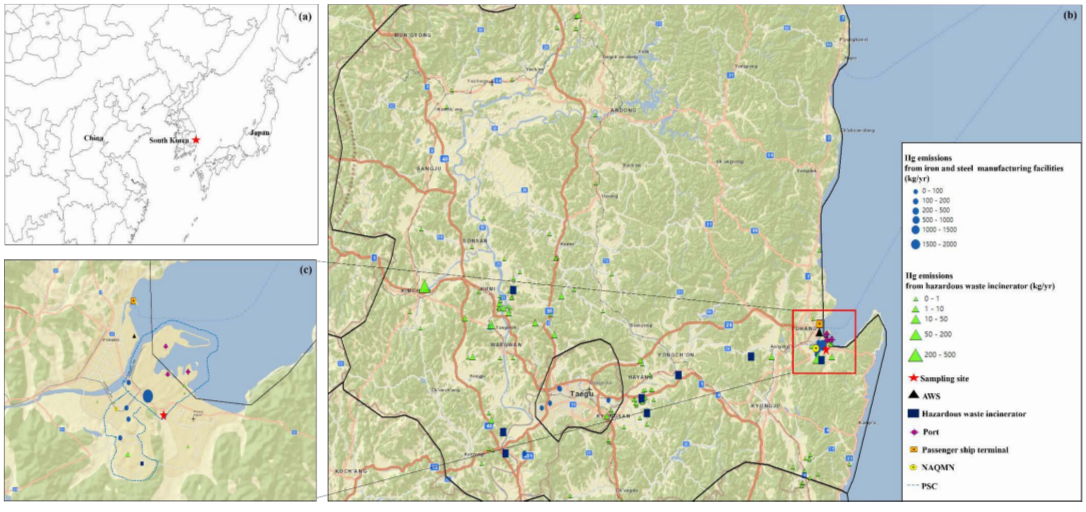

473

Fig. 1. The location of sampling site in this study ((a) South Korea, (b) Gyeongsangbuk-do and (c) Pohang). AWS, NAQMN and PSC represent Automatic Weather Station, National Air Quality Monitoring Network and Pohang Steel Complex, respectively.

Atmos. Chem. Phys. Discuss., doi:10.5194/acp-2015-939, 2016
Manuscript under review for journal Atmos. Chem. Phys.
Published: 18 January 2016

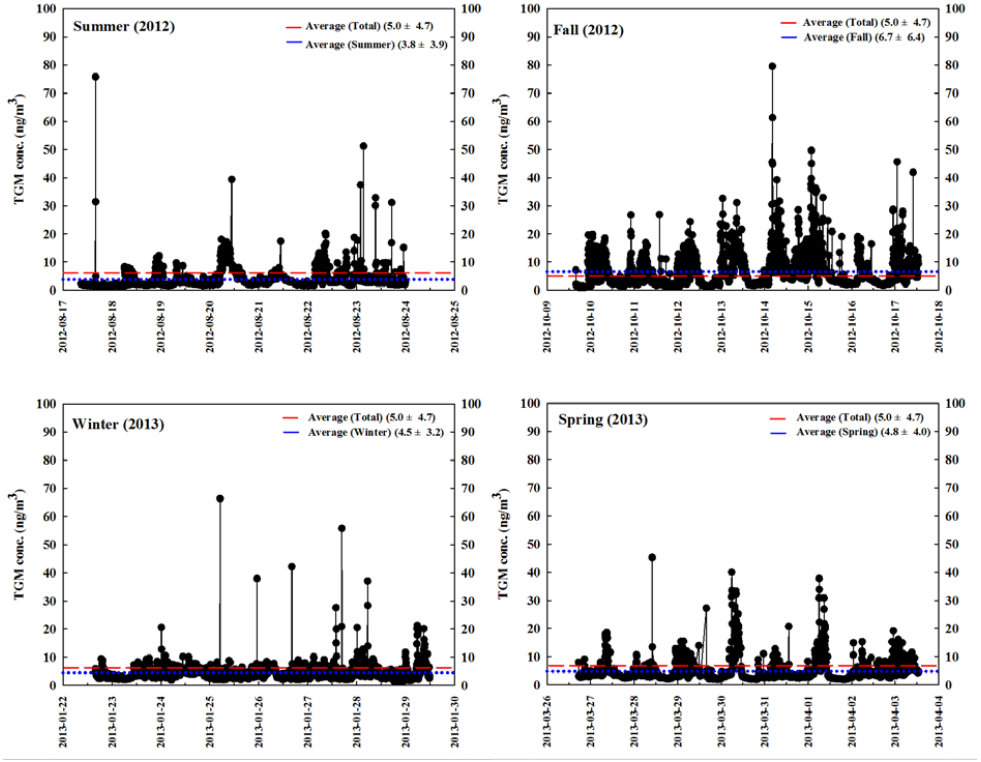

Fig. 2. Time-series of TGM concentrations in this study.

Atmos. Chem. Phys. Discuss., doi:10.5194/acp-2015-939, 2016
Manuscript under review for journal Atmos. Chem. Phys.
Published: 18 January 2016

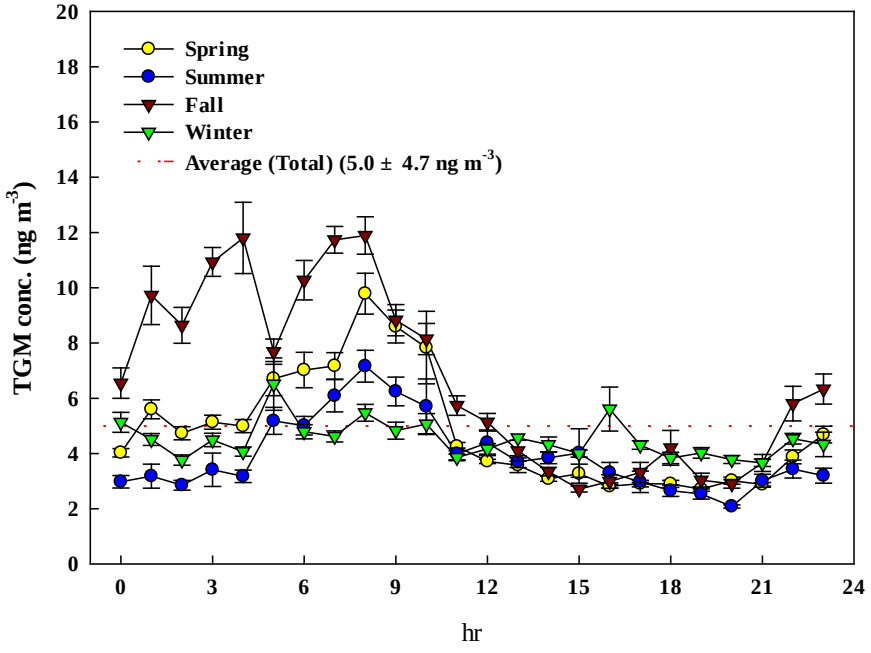

Fig. 3. The diurnal variations of TGM concentrations during the sampling periods. The error bars represent standard error.

Atmos. Chem. Phys. Discuss., doi:10.5194/acp-2015-939, 2016
Manuscript under review for journal Atmos. Chem. Phys.
Published: 18 January 2016

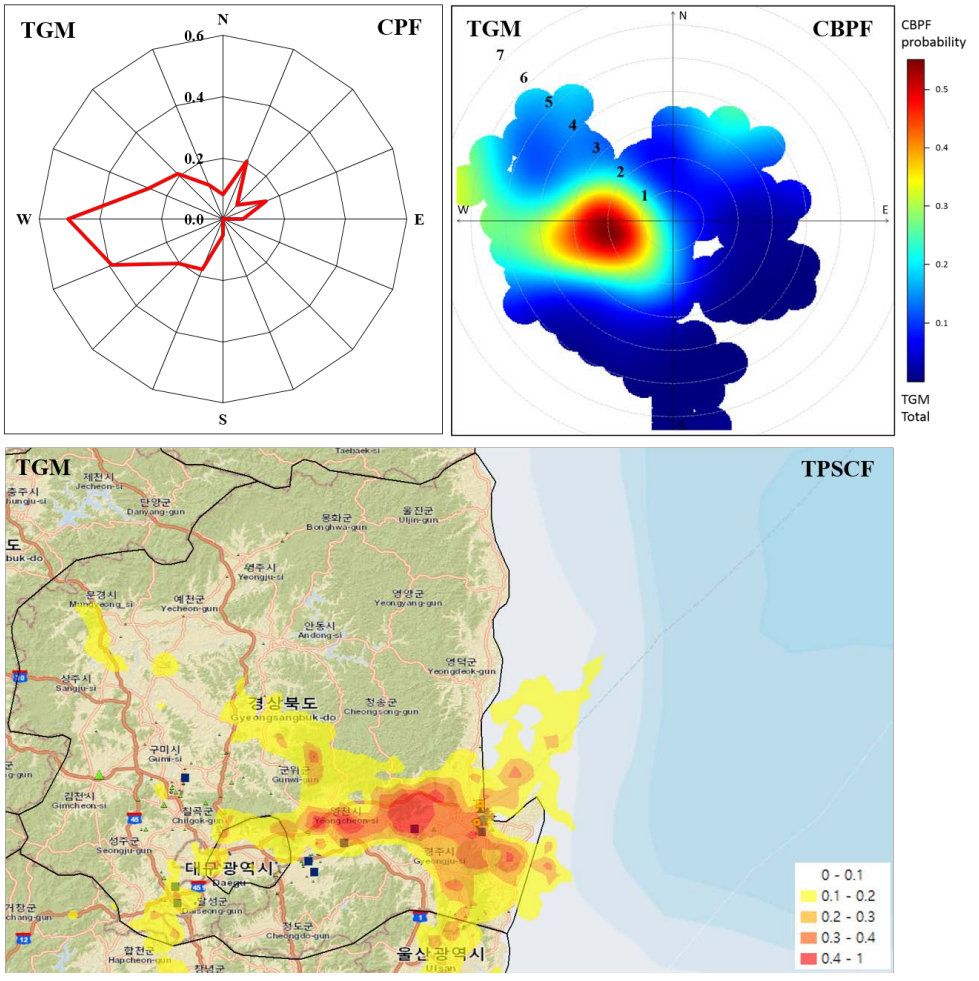

Fig. 4. CPF, CBPF and TPSCF plots for TGM higher than average concentration. The radial axes of CPF and CBPF are the probability and the wind speed (m s^{-1}), respectively.

Atmos. Chem. Phys. Discuss., doi:10.5194/acp-2015-939, 2016
Manuscript under review for journal Atmos. Chem. Phys.
Published: 18 January 2016

Atmospheric Chemistry and Physics Discussions

References

Adame, J., Notario, A., Villanueva, F., and Albaladejo, J.: Application of cluster analysis to surface ozone, NO_2 and SO_2 daily patterns in an industrial area in Central-Southern Spain measured with a DOAS system, Sci. Total Environ., 429**,** 281-291, 2012.

Amyot, M., Mcqueen, D. J., Mierle, G., and Lean, D. R.: Sunlight-induced formation of dissolved gaseous mercury in lake waters, Environ. Sci. Technol., 28**,** 2366-2371, 1994.

Ashbaugh, L. L., Malm, W. C., and Sadeh, W. Z.: A residence time probability analysis of sulfur concentrations at Grand Canyon National Park, Atmospheric Environment (1967), 19**,** 1263-1270, 1985.

Begum, B. A., Kim, E., Biswas, S. K., and Hopke, P. K.: Investigation of sources of atmospheric aerosol at urban and semi-urban areas in Bangladesh, Atmos. Environ., 38**,** 3025-3038, 2004.

Cheng, I., Zhang, L., Mao, H., Blanchard, P., Tordon, R., and Dalziel, J.: Seasonal and diurnal patterns of speciated atmospheric mercury at a coastal-rural and a coastal-urban site, Atmos. Environ., 82**,** 193-205, 2014.

Cheng, M. D., Hopke, P. K., and Zeng, Y.: A receptor-oriented methodology for determining source regions of particulate sulfate observed at Dorset, Ontario, Journal of Geophysical Research: Atmospheres (1984–2012), 98**,** 16839-16849, 1993.

Choi, E.-M., Kim, S.-H., Holsen, T. M., and Yi, S.-M.: Total gaseous concentrations in mercury in Seoul, Korea: local sources compared to long-range transport from China and Japan, Environ. Pollut., 157**,** 816-822, 2009.

Choi, E., Heo, J.-B., Hopke, P. K., Jin, B.-B., and Yi, S.-M.: Identification, apportionment, and photochemical reactivity of non-methane hydrocarbon sources in Busan, Korea, Water, Air, Soil Pollut., 215**,** 67-82, 2011.

Choi, H.-D., Huang, J., Mondal, S., and Holsen, T. M.: Variation in concentrations of three mercury (Hg) forms at a rural and a suburban site in New York State, Sci. Total Environ., 448**,** 96-106, 2013.

Dommergue, A., Ferrari, C. P., Planchon, F. A., and Boutron, C. F.: Influence of anthropogenic sources on total gaseous mercury variability in Grenoble suburban air (France), Sci. Total Environ., 297**,** 203-213, 2002.

Dvonch, J., Graney, J., Marsik, F., Keeler, G., and Stevens, R.: An investigation of source–receptor relationships for mercury in south Florida using event precipitation data, Sci. Total Environ., 213**,** 95-108, 1998.

Fang, F., Wang, Q., and Li, J.: Urban environmental mercury in Changchun, a metropolitan city in Northeastern China: source, cycle, and fate, Sci. Total Environ., 330**,** 159-170, 2004.

Feng, X., Shang, L., Wang, S., Tang, S., and Zheng, W.: Temporal variation of total gaseous mercury in the air of Guiyang, China, Journal of Geophysical Research: Atmospheres (1984–2012), 109, 2004.

Flanders, J., Turner, R., Morrison, T., Jensen, R., Pizzuto, J., Skalak, K., and Stahl, R.: Distribution, behavior, and transport of inorganic and methylmercury in a high gradient stream, Appl. Geochem., 25**,** 1756-1769, 2010.

Friedli, H., Arellano Jr, A., Geng, F., Cai, C., and Pan, L.: Measurements of atmospheric mercury in Shanghai during September 2009, Atmospheric Chemistry and Physics, 11**,** 3781-3788, 2011.

Atmos. Chem. Phys. Discuss., doi:10.5194/acp-2015-939, 2016
Manuscript under review for journal Atmos. Chem. Phys.
Published: 18 January 2016

Atmospheric Chemistry and Physics Discussions

531 Friedli, H. R., Radke, L. F., Prescott, R., Li, P., Woo, J. H., and Carmichael, G. R.: Mercury
532 in the atmosphere around Japan, Korea, and China as observed during the 2001 ACE-
533 Asia field campaign: Measurements, distributions, sources, and implications, Journal
534 of Geophysical Research: Atmospheres (1984–2012), 109, 2004.
535 Fu, X., Feng, X., Dong, Z., Yin, R., Wang, J., Yang, Z., and Zhang, H.: Atmospheric gaseous
536 elemental mercury (GEM) concentrations and mercury depositions at a high-altitude
537 mountain peak in south China, Atmospheric Chemistry and Physics, 10**,** 2425-2437,
538 2010.
539 Fu, X., Feng, X., Zhu, W., Wang, S., and Lu, J.: Total gaseous mercury concentrations in
540 ambient air in the eastern slope of Mt. Gongga, South-Eastern fringe of the Tibetan
541 plateau, China, Atmos. Environ., 42**,** 970-979, 2008.
542 Gauchard, P.-A., Ferrari, C. P., Dommergue, A., Poissant, L., Pilote, M., Guehenneux, G.,
543 Boutron, C. F., and Baussand, P.: Atmospheric particle evolution during a nighttime
544 atmospheric mercury depletion event in sub-Arctic at Kuujjuarapik/Whapmagoostui,
545 Quebec, Canada, Sci. Total Environ., 336**,** 215-224, 2005.
546 Gupta, A., Patil, R., and Gupta, S.: Emissions of gaseous and particulate pollutants in a port
547 and harbour region in India, Environ. Monit. Assess., 80**,** 187-205, 2002.
548 Han, Y.-J., Holsen, T. M., Hopke, P. K., Cheong, J.-P., Kim, H., and Yi, S.-M.: Identification
549 of source locations for atmospheric dry deposition of heavy metals during yellow-
550 sand events in Seoul, Korea in 1998 using hybrid receptor models, Atmos. Environ.,
551 38**,** 5353-5361, 2004.
552 Han, Y.-J., Holsen, T. M., Hopke, P. K., and Yi, S.-M.: Comparison between back-trajectory
553 based modeling and Lagrangian backward dispersion modeling for locating sources of
554 reactive gaseous mercury, Environ. Sci. Technol., 39**,** 1715-1723, 2005.
555 Heo, J.-B., Hopke, P., and Yi, S.-M.: Source apportionment of $PM_{2.5}$ in Seoul, Korea,
556 Atmospheric Chemistry and Physics, 9**,** 4957-4971, 2009.
557 Holmes, C. D., Jacob, D. J., Mason, R. P., and Jaffe, D. A.: Sources and deposition of
558 reactive gaseous mercury in the marine atmosphere, Atmos. Environ., 43**,** 2278-2285,
559 2009.
560 Hopke, P., Barrie, L., Li, S. M., Cheng, M. D., Li, C., and Xie, Y.: Possible sources and
561 preferred pathways for biogenic and non-sea-salt sulfur for the high Arctic, Journal of
562 Geophysical Research: Atmospheres (1984–2012), 100**,** 16595-16603, 1995.
563 Hopke, P. K.: Recent developments in receptor modeling, J. Chemometrics, 17**,** 255-265,
564 2003.
565 Hopke, P. K., Zhou, L., and Poirot, R. L.: Reconciling trajectory ensemble receptor model
566 results with emissions, Environ. Sci. Technol., 39**,** 7980-7983, 2005.
567 Hoyer, M., Burke, J., and Keeler, G. 1995. Atmospheric sources, transport and deposition of
568 mercury in Michigan: two years of event precipitation. *Mercury as a Global*
569 *Pollutant.* Springer.
570 Hsu, Y.-K., Holsen, T. M., and Hopke, P. K.: Comparison of hybrid receptor models to locate
571 PCB sources in Chicago, Atmos. Environ., 37**,** 545-562, 2003.
572 Huang, J., Choi, H.-D., Hopke, P. K., and Holsen, T. M.: Ambient mercury sources in
573 Rochester, NY: results from principle components analysis (PCA) of mercury
574 monitoring network data, Environ. Sci. Technol., 44**,** 8441-8445, 2010.
575 Iverfeldt, : Occurrence and turnover of atmospheric mercury over the Nordic countries, Water
576 Air & Soil Pollution, 56**,** 251-265, 1991.
577 Jaffe, D., Prestbo, E., Swartzendruber, P., Weiss-Penzias, P., Kato, S., Takami, A.,
578 Hatakeyama, S., and Kajii, Y.: Export of atmospheric mercury from Asia, Atmos.
579 Environ., 39**,** 3029-3038, 2005.

Atmos. Chem. Phys. Discuss., doi:10.5194/acp-2015-939, 2016
Manuscript under review for journal Atmos. Chem. Phys.
Published: 18 January 2016

Atmospheric Chemistry and Physics Discussions

580 Kellerhals, M., Beauchamp, S., Belzer, W., Blanchard, P., Froude, F., Harvey, B., Mcdonald,
581 K., Pilote, M., Poissant, L., and Puckett, K.: Temporal and spatial variability of total
582 gaseous mercury in Canada: results from the Canadian Atmospheric Mercury
583 Measurement Network (CAMNet), Atmos. Environ., 37**,** 1003-1011, 2003.
584 Kim, E., Hopke, P. K., and Edgerton, E. S.: Source identification of Atlanta aerosol by
585 positive matrix factorization, J. Air Waste Manage. Assoc., 53**,** 731-739, 2003a.
586 Kim, E., Larson, T. V., Hopke, P. K., Slaughter, C., Sheppard, L. E., and Claiborn, C.: Source
587 identification of $PM_{2.5}$ in an arid Northwest US City by positive matrix factorization,
588 Atmospheric Research, 66**,** 291-305, 2003b.
589 Kim, J.-H., Park, J.-M., Lee, S.-B., Pudasainee, D., and Seo, Y.-C.: Anthropogenic mercury
590 emission inventory with emission factors and total emission in Korea, Atmos.
591 Environ., 44**,** 2714-2721, 2010.
592 Kim, K.-H., and Kim, M.-Y.: Some insights into short-term variability of total gaseous
593 mercury in urban air, Atmos. Environ., 35**,** 49-59, 2001.
594 Kim, S.-H., Han, Y.-J., Holsen, T. M., and Yi, S.-M.: Characteristics of atmospheric
595 speciated mercury concentrations (TGM, Hg (II) and Hg (p)) in Seoul, Korea, Atmos.
596 Environ., 43**,** 3267-3274, 2009.
597 Kuo, T.-H., Chang, C.-F., Urba, A., and Kvietkus, K.: Atmospheric gaseous mercury in
598 Northern Taiwan, Sci. Total Environ., 368**,** 10-18, 2006.
599 Lai, S.-O., Holsen, T. M., Hopke, P. K., and Liu, P.: Wet deposition of mercury at a New
600 York state rural site: concentrations, fluxes, and source areas, Atmos. Environ., 41**,**
601 4337-4348, 2007.
602 Laurier, F. J., Mason, R. P., Whalin, L., and Kato, S.: Reactive gaseous mercury formation in
603 the North Pacific Ocean's marine boundary layer: A potential role of halogen
604 chemistry, Journal of Geophysical Research: Atmospheres (1984–2012), 108, 2003.
605 Lee, D. S., Dollard, G. J., and Pepler, S.: Gas-phase mercury in the atmosphere of the United
606 Kingdom, Atmos. Environ., 32**,** 855-864, 1998.
607 Lee, S. J., Seo, Y.-C., Jurng, J., Hong, J.-H., Park, J.-W., Hyun, J. E., and Lee, T. G.:
608 Mercury emissions from selected stationary combustion sources in Korea, Sci. Total
609 Environ., 325**,** 155-161, 2004.
610 Li, Z., Xia, C., Wang, X., Xiang, Y., and Xie, Z.: Total gaseous mercury in Pearl River Delta
611 region, China during 2008 winter period, Atmos. Environ., 45**,** 834-838, 2011.
612 Lim, C.-J., Cheng, M.-D., and Schroeder, W. H.: Transport patterns and potential sources of
613 total gaseous mercury measured in Canadian high Arctic in 1995, Atmos. Environ.,
614 35**,** 1141-1154, 2001.
615 Lin, C.-J., and Pehkonen, S. O.: The chemistry of atmospheric mercury: a review, Atmos.
616 Environ., 33**,** 2067-2079, 1999.
617 Lin, C.-J., Pongprueksa, P., Lindberg, S. E., Pehkonen, S. O., Byun, D., and Jang, C.:
618 Scientific uncertainties in atmospheric mercury models I: Model science evaluation,
619 Atmos. Environ., 40**,** 2911-2928, 2006.
620 Lindberg, S., Bullock, R., Ebinghaus, R., Engstrom, D., Feng, X., Fitzgerald, W., Pirrone, N.,
621 Prestbo, E., and Seigneur, C.: A synthesis of progress and uncertainties in attributing
622 the sources of mercury in deposition, AMBIO: A Journal of the Human Environment,
623 36**,** 19-33, 2007.
624 Liu, N., Qiu, G., Landis, M. S., Feng, X., Fu, X., and Shang, L.: Atmospheric mercury
625 species measured in Guiyang, Guizhou province, southwest China, Atmospheric
626 Research, 100**,** 93-102, 2011.
627 Lu, J. Y., and Schroeder, W. H.: Annual time-series of total filterable atmospheric mercury
628 concentrations in the Arctic, Tellus B, 56**,** 213-222, 2004.

Atmos. Chem. Phys. Discuss., doi:10.5194/acp-2015-939, 2016
Manuscript under review for journal Atmos. Chem. Phys.
Published: 18 January 2016

Atmospheric Chemistry and Physics Discussions

629 Lynam, M. M., and Keeler, G. J.: Source–receptor relationships for atmospheric mercury in
630 urban Detroit, Michigan, Atmos. Environ., 40**,** 3144-3155, 2006.
631 Mao, H., Talbot, R., Sigler, J., Sive, B., and Hegarty, J.: Seasonal and diurnal variations of
632 Hg over New England, Atmospheric Chemistry and Physics, 8**,** 1403-1421, 2008.
633 Mason, R. P., and Sheu, G. R.: Role of the ocean in the global mercury cycle, Global
634 biogeochemical cycles, 16**,** 40-1-40-14, 2002.
635 Miller, C. L., Watson, D. B., Lester, B. P., Lowe, K. A., Pierce, E. M., and Liang, L.:
636 Characterization of soils from an industrial complex contaminated with elemental
637 mercury, Environ. Res., 125**,** 20-29, 2013.
638 Nakagawa, R.: Studies on the levels in atmospheric concentrations of mercury in Japan,
639 Chemosphere, 31**,** 2669-2676, 1995.
640 Nier: National Air Pollutants Emission 2011 (in Korean), 2011.
641 Obrist, D., Tas, E., Peleg, M., Matveev, V., Faïn, X., Asaf, D., and Luria, M.: Bromine-
642 induced oxidation of mercury in the mid-latitude atmosphere, Nature Geoscience, 4**,**
643 22-26, 2011.
644 Osawa, T., Ueno, T., and Fu, F.: Sequential variation of atmospheric mercury in Tokai-mura,
645 seaside area of eastern central Japan, Journal of Geophysical Research: Atmospheres
646 (1984–2012), 112, 2007.
647 Pacyna, E. G., Pacyna, J. M., Steenhuisen, F., and Wilson, S.: Global anthropogenic mercury
648 emission inventory for 2000, Atmos. Environ., 40**,** 4048-4063, 2006.
649 Pirrone, N., Cinnirella, S., Feng, X., Finkelman, R., Friedli, H., Leaner, J., Mason, R.,
650 Mukherjee, A., Stracher, G., and Streets, D.: Global mercury emissions to the
651 atmosphere from anthropogenic and natural sources, Atmospheric Chemistry and
652 Physics, 10**,** 5951-5964, 2010.
653 Poissant, L.: Potential sources of atmospheric total gaseous mercury in the St. Lawrence
654 River valley, Atmos. Environ., 33**,** 2537-2547, 1999.
655 Polissar, A. V., Hopke, P. K., and Harris, J. M.: Source regions for atmospheric aerosol
656 measured at Barrow, Alaska, Environ. Sci. Technol., 35**,** 4214-4226, 2001.
657 Sakata, M., and Marumoto, K.: Formation of atmospheric particulate mercury in the Tokyo
658 metropolitan area, Atmos. Environ., 36**,** 239-246, 2002.
659 Sakata, M., and Marumoto, K.: Wet and dry deposition fluxes of mercury in Japan, Atmos.
660 Environ., 39**,** 3139-3146, 2005.
661 Schmeltz, D., Evers, D. C., Driscoll, C. T., Artz, R., Cohen, M., Gay, D., Haeuber, R.,
662 Krabbenhoft, D. P., Mason, R., and Morris, K.: MercNet: a national monitoring
663 network to assess responses to changing mercury emissions in the United States,
664 Ecotoxicology, 20**,** 1713-1725, 2011.
665 Schmolke, S. R., Schroeder, W., Kock, H., Schneeberger, D., Munthe, J., and Ebinghaus, R.:
666 Simultaneous measurements of total gaseous mercury at four sites on a 800km
667 transect: spatial distribution and short-time variability of total gaseous mercury over
668 central Europe, Atmos. Environ., 33**,** 1725-1733, 1999.
669 Schroeder, W. H., and Munthe, J.: Atmospheric mercury—an overview, Atmos. Environ., 32**,**
670 809-822, 1998.
671 Seo, Y.-S., Han, Y.-J., Holsen, T. M., Choi, E., Zoh, K.-D., and Yi, S.-M.: Source
672 identification of total mercury (TM) wet deposition using a Lagrangian particle
673 dispersion model (LPDM), Atmos. Environ., 104**,** 102-111, 2015.
674 Shon, Z.-H., Kim, K.-H., Kim, M.-Y., and Lee, M.: Modeling study of reactive gaseous
675 mercury in the urban air, Atmos. Environ., 39**,** 749-761, 2005.
676 Song, X., Cheng, I., and Lu, J.: Annual atmospheric mercury species in downtown Toronto,
677 Canada, J. Environ. Monit., 11**,** 660-669, 2009.

Atmos. Chem. Phys. Discuss., doi:10.5194/acp-2015-939, 2016
Manuscript under review for journal Atmos. Chem. Phys.
Published: 18 January 2016

Atmospheric Chemistry and Physics Discussions

678 Sprovieri, F., Pirrone, N., Ebinghaus, R., Kock, H., and Dommergue, A.: A review of
679 worldwide atmospheric mercury measurements, Atmospheric Chemistry and Physics,
680 10**,** 8245-8265, 2010.
681 Stamenkovic, J., Lyman, S., and Gustin, M. S.: Seasonal and diel variation of atmospheric
682 mercury concentrations in the Reno (Nevada, USA) airshed, Atmos. Environ., 41**,**
683 6662-6672, 2007.
684 Uria-Tellaetxe, I., and Carslaw, D. C.: Conditional bivariate probability function for source
685 identification, Environ. Model. Software, 59**,** 1-9, 2014.
686 Wan, Q., Feng, X., Lu, J., Zheng, W., Song, X., Han, S., and Xu, H.: Atmospheric mercury in
687 Changbai Mountain area, northeastern China I. The seasonal distribution pattern of
688 total gaseous mercury and its potential sources, Environ. Res., 109**,** 201-206, 2009.
689 Weiss-Penzias, P., Jaffe, D., Swartzendruber, P., Hafner, W., Chand, D., and Prestbo, E.:
690 Quantifying Asian and biomass burning sources of mercury using the Hg/CO ratio in
691 pollution plumes observed at the Mount Bachelor Observatory, Atmos. Environ., 41**,**
692 4366-4379, 2007.
693 Weiss-Penzias, P., Jaffe, D. A., Mcclintick, A., Prestbo, E. M., and Landis, M. S.: Gaseous
694 elemental mercury in the marine boundary layer: Evidence for rapid removal in
695 anthropogenic pollution, Environ. Sci. Technol., 37**,** 3755-3763, 2003.
696 Weiss-Penzias, P., Jaffe, D. A., Swartzendruber, P., Dennison, J. B., Chand, D., Hafner, W.,
697 and Prestbo, E.: Observations of Asian air pollution in the free troposphere at Mount
698 Bachelor Observatory during the spring of 2004, Journal of Geophysical Research:
699 Atmospheres (1984–2012), 111, 2006.
700 Xie, Y., and Berkowitz, C. M.: The use of positive matrix factorization with conditional
701 probability functions in air quality studies: an application to hydrocarbon emissions in
702 Houston, Texas, Atmos. Environ., 40**,** 3070-3091, 2006.
703 Zeng, Y., and Hopke, P.: A study of the sources of acid precipitation in Ontario, Canada,
704 Atmospheric Environment (1967), 23**,** 1499-1509, 1989.
705 Zhang, H., and Lindberg, S. E.: Sunlight and iron (III)-induced photochemical production of
706 dissolved gaseous mercury in freshwater, Environ. Sci. Technol., 35**,** 928-935, 2001.
707 Zhao, W., Hopke, P. K., and Karl, T.: Source identification of volatile organic compounds in
708 Houston, Texas, Environ. Sci. Technol., 38**,** 1338-1347, 2004.
709 Zhou, L., Kim, E., Hopke, P. K., Stanier, C. O., and Pandis, S.: Advanced factor analysis on
710 Pittsburgh particle size-distribution data special issue of aerosol science and
711 technology on findings from the Fine Particulate Matter Supersites Program, Aerosol
712 Science and Technology, 38**,** 118-132, 2004.
713 Zhu, J., Wang, T., Talbot, R., Mao, H., Hall, C., Yang, X., Fu, C., Zhuang, B., Li, S., and
714 Han, Y.: Characteristics of atmospheric total gaseous mercury (TGM) observed in
715 urban Nanjing, China, Atmospheric Chemistry and Physics, 12**,** 12103-12118, 2012.